An effective approach based on reliability methods for high-dimensional Bayesian model updating of dynamical nonlinear structures

D. J. Jerez[1], H. J. Jensen[2], M. Beer[1,3,4], and C. Figueroa[2]

[1] Institute for Risk and Reliability, Leibniz University Hannover, Hannover, Germany
[2] Civil Engineering Department, Federico Santa Maria Technical University, Valparaiso, Chile
[3] International Joint Research Center for Engineering Reliability and Stochastic Mechanics, Tongji University, Shanghai, China
[4] Institute for Risk and Uncertainty and School of Engineering, University of Liverpool, Liverpool, United Kingdom

E-mail: danko.jerez@irz.uni-hannover.de

Abstract. Bayesian model updating represents a sound formulation to incorporate the unavoidable uncertainties arising in the system identification of infrastructure assets. However, the treatment of cases involving a relatively large number of model parameters remains an open issue, especially for dynamic nonlinear structural models. In this context, an effective implementation of subset simulation is considered within the framework of Bayesian model updating with structural reliability methods (BUS). For improved numerical efficiency, a substructure coupling technique for dynamic analysis is implemented to develop a reduced-order model strategy. To assess the capabilities of the proposed method, an application example that considers a three-dimensional bridge model equipped with nonlinear devices is presented.

1. Introduction

The evaluation of the state of structural dynamical systems using measured responses is an important and current challenge in civil engineering. The treatment of the inherent uncertainties arising in this context is of paramount importance, for which Bayesian model updating yields a suitable probabilistic formulation [1, 2]. In this setting, the updated joint distribution of the uncertain parameters is obtained taking into account available measurements as well as prior knowledge. For problems involving a large amount of data, asymptotic methods can be used to obtain explicit approximations of the posterior distribution [1, 3]. In more general cases, posterior samples can be generated by applying specialized stochastic simulation methods. Some available techniques include, e.g., the Metropolis-Hastings (M-H) algorithm [4, 5] and the transitional Markov chain Monte Carlo (TMCMC) method [6]. While these sampling approaches have been demonstrated in different applications (see, e.g., [7, 8]), they face potential problems when the number of identification parameters is relatively high [9, 10].

Some approaches to explore high-dimensional posterior distributions of structural dynamical models include Hamiltonian Monte Carlo [10], subspace identification techniques [11], and the use of Kalman filters [12]. From a general perspective, the suitability of the different solution techniques is heavily dependent on the particularities of the problem at hand. Thus, it can be

argued that there is still room for additional advancements in this field. In this regard, one type of approaches that can potentially handle high-dimensional parameter spaces corresponds to Bayesian model updating using structural reliability methods (BUS) [13, 14, 15, 16]. The distinctive feature of BUS is that an auxiliary reliability problem is formulated to explore the target posterior distribution. In this regard, the corresponding failure event can be defined a priori [13, 15] or adaptively during the sample generation process [14, 16, 17]. Even though these techniques have been implemented in a number of applications [18, 19], their use in structural dynamics applications involving complex nonlinear models and response measurements remains rather limited.

This contribution presents a BUS approach for identification problems involving dynamic nonlinear structures and measured response data. A strategy based on subset simulation [20] is formulated, which requires minimal modifications to the original algorithm and circumvents the need of knowledge about the maximum likelihood value. Several implementation aspects are discussed to enhance the effectiveness of the method. Overall, the resulting method is a potentially useful tool to address Bayesian updating problems that involve structural dynamical models with high-dimensional parameter spaces.

2. Problem formulation

2.1. Bayesian model updating

Consider model parameter vector $\boldsymbol{\theta} \in \boldsymbol{\Theta} \subset \mathbb{R}^{n_\theta}$ corresponding to a model class M and available measurement data denoted by D. The goal of Bayesian model updating is to characterize the updated joint distribution of $\boldsymbol{\theta}$, i.e., $p(\boldsymbol{\theta}|D)$. From Bayes' theorem [1, 2],

$$p(\boldsymbol{\theta}|D) = \frac{p(\boldsymbol{\theta})L_D(\boldsymbol{\theta})}{P(D)} \tag{1}$$

where $p(\boldsymbol{\theta})$ denotes the prior probability density function (PDF), $L_D(\boldsymbol{\theta})$ is the likelihood function, and $P(D) = \int p(\boldsymbol{\theta})L_D(\boldsymbol{\theta})d\boldsymbol{\theta}$ is the so-called evidence. The initial knowledge about the plausibility of different model parameter values is incorporated by means of $p(\boldsymbol{\theta})$. Further, $L_D(\boldsymbol{\theta})$ quantifies how likely is to observe the available measurements for a given parameter vector $\boldsymbol{\theta}$. Finally, $P(D)$ is a normalizing constant.

2.2. Likelihood function

This contribution focuses on structural dynamical systems in which the identification data D comprises time series of length n_t corresponding to a total of n_η responses of interest. Specifically, $\eta_n^*(t_j)$ denotes the nth response of interest measured at time t_j with $n = 1, \ldots, n_\eta$ and $j = 1, \ldots, n_t$, while $\eta_n(t_j, \boldsymbol{\theta})$ is the associated prediction corresponding to the parameter vector $\boldsymbol{\theta}$. Further, the prediction errors $e_{n,j}(\boldsymbol{\theta}) = \eta_n^*(t_j) - \eta_n(t_j, \boldsymbol{\theta})$ are assumed to be independent random variables that follow a zero-mean Gaussian distribution with variance equal to σ^2. Then, it is possible to state the likelihood function as [1]

$$L_D(\boldsymbol{\theta}) = \frac{1}{(2\pi\sigma^2)^{n_\eta n_t/2}} \exp\left[-\frac{1}{2\sigma^2}\sum_{n=1}^{n_\eta}\sum_{j=1}^{n_t}\left(\eta_n^*(t_j) - \eta_n(t_j, \boldsymbol{\theta})\right)^2\right] \tag{2}$$

2.3. Structural dynamical systems

Special attention is directed to structural systems characterized as multi-degree-of-freedom models whose response satisfies the equation of motion

$$\mathbf{M}\ddot{\mathbf{y}}(t) + \mathbf{C}\dot{\mathbf{y}}(t) + \mathbf{K}\mathbf{y}(t) + \boldsymbol{\kappa}(\dot{\mathbf{y}}(t), \mathbf{y}(t), \boldsymbol{\zeta}(t)) = \mathbf{f}(t) \tag{3}$$

where $\mathbf{y} \in \mathbb{R}^{n_y}$ is the displacement vector; the matrices $\mathbf{M}$ is the mass matrix; $\mathbf{C}$ is the damping matrix; $\mathbf{K}$ is the stiffness matrix; $\mathbf{f}(t)$ denotes the vector of external forces; and $\boldsymbol{\kappa}(\dot{\mathbf{y}}(t), \mathbf{y}(t), \boldsymbol{\zeta}(t))$ is a vector comprising the nonlinear forces of the system, whose state variables $\boldsymbol{\zeta}(t)$ satisfy an appropriate nonlinear equation. Although Eq. (3) is particularly well suited to treat localized nonlinearities, it can also be extended to consider nonlinear models of the entire structure. Finally, it is noted that the evaluation of $\eta_n(t_j, \boldsymbol{\theta})$, $n = 1, \ldots, n_\eta$, $j = 1, \ldots, n_t$ requires solving coupled nonlinear differential equations to determine the joint evolution of $\mathbf{y}(t)$ and $\boldsymbol{\zeta}(t)$. This can be carried out by resorting to any appropriate numerical technique.

3. Solution method

3.1. Equivalent formulation based on reliability problems

The main idea of BUS is to formulate Bayesian model updating as the equivalent task of characterizing a suitable failure domain [13]. In this regard, consider the auxiliary failure event

$$Z = \{u < cL_D(\boldsymbol{\theta})\} \tag{4}$$

where $u \in [0, 1]$ is a uniform random variable, $\boldsymbol{\theta} \in \boldsymbol{\Theta} \subseteq \mathbb{R}^{n_\theta}$ follows the prior distribution $p(\boldsymbol{\theta})$ in Eq. (1), and $c > 0$ is referred to as the likelihood multiplier. This constant verifies [13]

$$c^{-1} \geq L_{\max} = \sup_{\boldsymbol{\theta} \in \boldsymbol{\Theta}} L_D(\boldsymbol{\theta}) \tag{5}$$

If the previous condition is satisfied, the marginal PDF of $\boldsymbol{\theta}$ given failure matches the posterior PDF in Eq. (1), that is, $p(\boldsymbol{\theta}|F) = p(\boldsymbol{\theta}|D)$. In other words, if failure samples $(\boldsymbol{\theta}, u) \sim p(\boldsymbol{\theta}, u|F)$ have been drawn using a suitable reliability method, their corresponding $\boldsymbol{\theta}$-components are distributed according to $p(\boldsymbol{\theta}|D)$. Finally, the evidence is obtained as $P(D) = c^{-1}P_F$, where P_F is the failure probability. This is a valuable feature for problems involving multiple probabilistic model classes [21].

3.2. Likelihood multiplier

The treatment of the likelihood multiplier is a key aspect of BUS. In practice, the optimal value choice $c^{-1} = L_{\max}$ cannot be guaranteed. While selecting $c^{-1} > L_{\max}$ ensures the validity of the formulation, if c^{-1} is too large the computational efforts might be excessive. Finally, in case $c^{-1} < L_{\max}$ the marginal conditional distribution $p(\boldsymbol{\theta}|F)$ becomes a biased version of the posterior PDF [15], that is, $p(\boldsymbol{\theta}|F) \neq p(\boldsymbol{\theta}|D)$. In this regard, several approaches have been proposed to select the value of c^{-1}. A straightforward strategy is to define c^{-1} a priori based on the characteristics of $L_D(\boldsymbol{\theta})$ [13], which can be complemented with a post-processing step [15]. Alternatively, adaptive schemes to select the likelihood multiplier based on intermediate results of the corresponding reliability analysis have been presented. Subset simulation [20] has been adopted to this end using an inner-outer approach [14] or an adaptive target failure event [16, 17]. In general, c^{-1} should be as small as possible while satisfying $c^{-1} \geq L_{\max}$.

3.3. Main ideas

In this work, a subset simulation-based strategy is developed to select the likelihood multiplier in an adaptive manner [17]. In this context, and taking into account the discussion in [14, 16], Eq. (4) is restated as

$$F = \{d(\boldsymbol{\theta}, u) > d^*\} = \left\{\ln\left(L_D(\boldsymbol{\theta})\right) - \ln\left(u\right) > \ln\left(c^{-1}\right)\right\} \tag{6}$$

where $d(\boldsymbol{\theta}, u) = \ln\left(L_D(\boldsymbol{\theta})\right) - \ln\left(u\right)$ is the equivalent demand function with threshold $d^* = \ln(c^{-1})$. Based on the previous formulation, subset simulation can be carried out without specifying the value of c^{-1} beforehand. Further, the value of d^* can be updated at the end of each sampling

stage using the maximum observed log-likelihood value. The conventional condition to stop the sampling process within subset simulation is implemented, i.e., the process is finished when the next intermediate threshold surpasses d^*. Hence, the herein proposed scheme only involves slight modifications to the customary subset simulation algorithm for its implementation. In addition, it is noted that the likelihood multiplier is explicitly selected as the maximum likelihood value observed throughout the entire sampling process.

3.4. Basic pseudo-code

For completeness, a pseudo-code of the proposed method is presented in the following. A more thorough description of the approach, which encompasses theoretical and practical implementation aspects, can be found in [17].

1. Define the conditional probability p_0 and the sample size N such that $p_0 N$ is integer.
2. Obtain a set of N samples, $\left\{(\boldsymbol{\theta}_n^0, u_n^0), n = 1, \ldots, N\right\}$ according to the unconditional distribution $p(\boldsymbol{\theta}, u)$. Evaluate the corresponding log-likelihood values $\ell_n^0 = \ln\left(L_D(\boldsymbol{\theta}_n^0, u_n^0)\right)$ and demand function values $d_n^0 = d(\boldsymbol{\theta}_n^0, u_n^0)$, $n = 1, \ldots, N$.
3. Initialize $k = 1$ and $d^* = \max_{n=1,\ldots,N} \ell_n^0$.
4. Set d^k as the $[(1 - p_0)N]$th largest value within $\{d_n^{k-1}, n = 1, \ldots, N\}$. If $d^k \geq d^*$, set $m = k$, $d^m = d^*$ and go to step 7. Otherwise, define the kth intermediate failure domain as $F_k = \{(\boldsymbol{\theta}, u) \in \boldsymbol{\Theta} \times [0, 1] : d(\boldsymbol{\theta}, u) > d^k\}$.
5. By construction, there are $p_0 N$ samples in $\left\{(\boldsymbol{\theta}_n^{k-1}, u_n^{k-1}), n = 1, \ldots, N\right\}$ that belong to F_k. Considering each sample as the seed state, employ the modified MH algorithm [20] to draw $(1 - p_0)N$ additional samples within F_k to obtain a set of N conditional samples $\left\{(\boldsymbol{\theta}_n^k, u_n^k), n = 1, \ldots, N\right\}$ at level k. The corresponding log-likelihood and demand function values are, respectively, $\ell_n^k = \ln\left(L_D(\boldsymbol{\theta}_n^k)\right)$ and $d_n^k = d(\boldsymbol{\theta}_n^k, u_n^k)$, $n = 1, \ldots, N$.
6. Update the threshold as $d^* \leftarrow \max\{d^*, \max_{n=1,\ldots,N} \ell_n^k\}$. Set $k \leftarrow k + 1$ and go back to step 4.
7. The set $\{\boldsymbol{\theta}_n^m, n = 1, \ldots, N\} \in F_m$ represent posterior samples. The evidence is estimated as

$$P(D) \approx e^{d^*} \times p_0^{m-1} \times \left(\frac{1}{N} \sum_{n=1}^{N} I\left[d(\boldsymbol{\theta}_n^m, u_n^m) > d^*\right] \right) \tag{7}$$

where $I[\cdot] = 1$ if the expression within square brackets is true and $I[\cdot] = 0$ otherwise.

3.5. Implementation details

The proposed approach can be regarded as computationally very demanding due to the significant number of dynamic analyses involved in its practical application. Some efficiency enhancements can be achieved by improving the effectiveness of the sampling process, such as the use of adaptive proposal distributions [22] or a resampling step to reduce sample dependency [16]. However, reducing the computational cost of evaluating $L_D(\boldsymbol{\theta})$ is paramount to enhance the numerical efficiency of the approach. In this regard, two different strategies are considered.

3.5.1. Parametric reduced-order models The concept of substructure coupling for dynamic analysis is employed to formulate a model reduction strategy within the herein proposed approach [23]. In this regard, a number of linear and nonlinear substructures are defined to characterize the whole structure, which are then coupled to obtain a model of reduced dimension. To circumvent the need of repeatedly assembling the different substructures, an efficient parametrization technique is implemented. In this setting, by assuming that the dynamical

matrices of each linear substructure can be parametrized in terms of a single parameter, the reduced-order matrices are explicitly parameterized in terms of the model parameters under consideration [24]. In general, significant computational savings can be achieved with this strategy.

3.5.2. Surrogate model strategies Additional efficiency improvements can be achieved by reducing the number of calls to the likelihood function. To this end, surrogate model strategies can be implemented [25] to approximate $L_D(\boldsymbol{\theta})$. The idea is to formulate a metamodel for the likelihood function based on, e.g., neural networks, support vector machines, or kriging interpolants. Ideally, a significant portion of the samples are evaluated using the metamodel instead of the likelihood function and, in this manner, the overall computational efficiency can be improved. An important implementation aspect is to achieve a suitable balance between the complexity of the metamodel and its accuracy. Even though surrogate modeling strategies can be very efficient for problems involving low-dimensional parameter spaces, their extension to cases with multiple uncertain parameters remains an open challenge.

4. Application example

4.1. Description of the structural system

The finite element model of a bridge structure, has been borrowed from [17] and is shown in Fig. 1, is considered in this work. The girder is supported by four piers of 8 m height with a rigid connection, where each of them rests on four piles of 35 m height. Such piles and piers are modeled by means of column elements whose cross sections are circular with diameters of 0.6 m and 1.6 m, respectively. Further, the total length of the deck is equal to 199 m across five spans. Shell and beam elements are implemented to characterize the deck cross section. In addition, a pair of sliding bearings is present at each abutment to support the bridge deck. These devices comprise a steel slider fixed at an upper plate that slides against a semi-spherical surface of stainless steel, thereby dissipating energy through friction-related phenomena [26]. Overall, approximately 10^5 degrees of freedom are involved in the dynamical characterization of the structural model.

For dynamic analysis purposes it is assumed that the nonlinearities are restricted to the response of the sliding bearings while the rest of structural components remain linear. An experimentally validated model is implemented to represent the nonlinear response of the bearings [26], thereby accounting for changes in the corresponding friction coefficient observed during seismic events. As an example, Fig. 2 shows a representative bearing response in terms of the relationship between restoring force and relative displacement. In addition, the structural elements are characterized by a Young modulus of 2.0×10^{10} N/m^2, a Poisson ratio of 0.2, and a mass density equal to 2500 kg/m^3. Further, a series of translational springs distributed along the height of the piles are employed to represent the interaction between the piles and their surrounding soil. The corresponding stiffness constants are assumed to grow linearly from 5.6×10^6 N/m at the surface to 1.1×10^8 N/m at the bottom of the piles. Finally, the critical damping ratio under consideration is equal to 3%.

4.2. Model reduction

The structural model is subdivided into sixteen linear structures and two nonlinear substructures as presented in Fig. 3. Specifically, the deck comprises substructures S_i, $i = 1, \ldots, 5$, the bridge piers correspond to substructures S_i, $i = 6, \ldots, 9$, and the corresponding footings and piles relate to substructures S_i, $i = 10, \ldots, 13$. Furthermore, the aforementioned springs that represent the interaction between piles and their surrounding soil conform substructures S_i, $i = 14, \ldots, 16$. Finally, substructures S_i, $i = 17, 18$ comprise the sliding bearings at the abutments. Thus, the

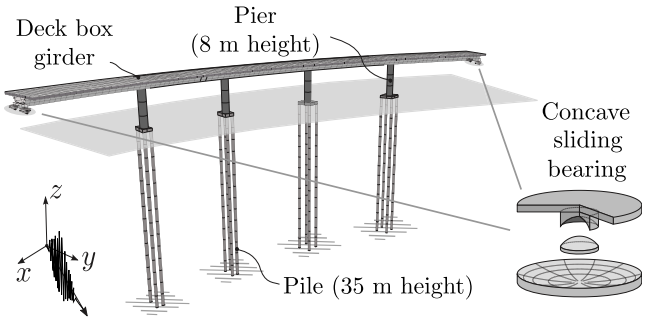

Figure 1. Three-dimensional representation of the bridge.

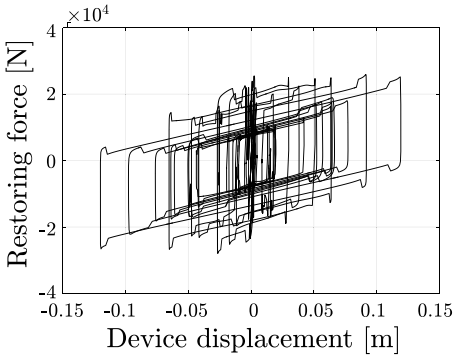

Figure 2. Typical bearing response.

linear substructures are S_i, $i = 1, \ldots, 16$, whereas substructures S_{17} and S_{18} are characterized as nonlinear.

A total of 449 generalized coordinates are obtained as a result of the above substructuring, which represents less than 5% of the total number of degrees of freedom involved in the unreduced finite element model. Moreover, additional analyses carried out in the context of this contribution determine errors in the ten lowest natural frequencies being smaller than 0.5%. It is noted that such frequencies account for the linear elements of the undamped structural system. In addition, Fig. 4 presents the modal assurance criterion (MAC) values [27] corresponding to mode shapes associated with the ten lowest natural frequencies of the unreduced and reduced-order systems. As the off-diagonal elements are negligible, both models can be considered consistent with respect to their mode shapes.

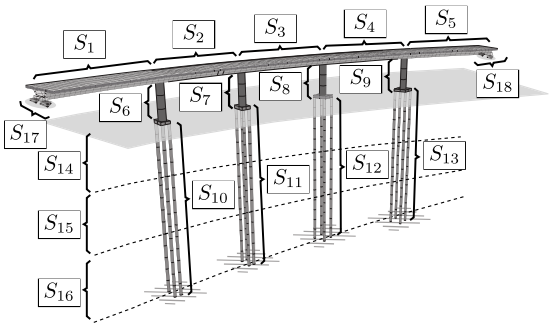

Figure 3. Selected substructures.

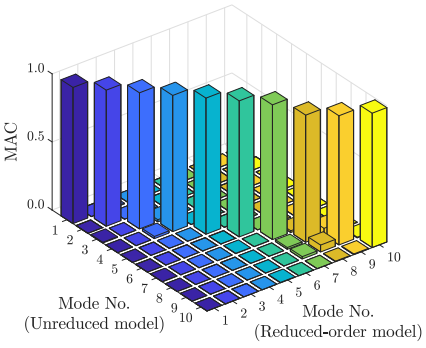

Figure 4. Resemblance of the mode shapes of original and reduced-order models in terms of their MAC values.

4.3. Identification problem

Synthetic measurement data are considered for identification purposes. The measurements are simulated by generating response time series with the nominal finite element model. To this end, El Centro ground-motion record has been applied at 50° with respect to the x axis and re-scaled so that the corresponding peak acceleration is equal to 5 m/s^2 (see Fig. 1). Synthetic acceleration measurements in the horizontal plane are considered for identification

purposes, which are obtained at the center of the different deck spans. A duration of 20 s with a time step $\Delta t = 0.01$ s is taken into account. To incorporate monitoring errors, a discrete white noise sequence is incorporated to contaminate the acceleration measurements. The corresponding standard deviation is taken equal to 10% of the root-mean-square value of the original acceleration responses ($\sigma_0 = 0.08$ m/s^2) Thus, the identification data comprises $n_r = 10$ responses of interest and $n_t = 2000$ time steps.

For illustration purposes, a total of five identification parameters are considered. In particular, θ_1 controls the elastic modulus of the deck girder, θ_2 of the piers, θ_3 of the pile elements, θ_4 is associated with the initial friction coefficient of the bearings, and θ_5 is related to σ in Eq. (2). These parameters are defined in a normalized way such that $\theta_i = 1$, $i = 1, \ldots, 5$, characterize the nominal (target) values. The prior PDF of θ_i, $i = 1, \ldots, 4$ is taken as uniform over $[0.5, 1.5]^4$, while the prior distribution of θ_5 is defined as lognormal with a median equal to 0.5 and a logarithmic standard deviation of 0.3.

Based on the previous formulation, it is possible to parametrize the different substructure stiffness matrices in terms of $\boldsymbol{\theta}$. In this regard, θ_1 is associated with substructures S_i, $i = 1, \ldots, 5$; θ_2 with S_i, $i = 6, \ldots, 9$; and θ_3 with S_i, $i = 10, \ldots, 13$. Hence, the strategy based on substructure coupling for dynamic analysis presented in Section 3.5.1 can be implemented. According to validation calculations, the speedup factor for evaluating $L_D(\boldsymbol{\theta})$ obtained by virtue of the aforementioned parametrization technique is approximately equal to 10 for this example.

4.4. Results

To generate a set of posterior samples, subset simulation is implemented with $N = 2000$ and $p_0 = 0.1$ (see Section 3.4). Table 1 shows the corresponding estimates of the posterior mean values. It is seen that the maximum deviation with respect to the target value $\theta_i^{target} = 1$, $i = 1, \ldots, 5$, is around 2%. It can be argued that such results are associated to the non-trivial interaction between the stiffness of the piers and piles, i.e., between parameters θ_2 and θ_3. That is, higher (lower) values of θ_2 can be compensated with lower (higher) values of θ_3 to obtain a similar dynamical behavior at the measurement points, which is consistent from the structural viewpoint.

Table 1. Posterior mean values of the identification parameters.

Parameter	Posterior mean value
θ_1	0.99
θ_2	1.02
θ_3	0.98
θ_4	1.00
θ_5	0.99

Table 2. Log-evidence estimates obtained in five algorithm runs.

Run No.	Log-evidence
1	2.21×10^{-4}
2	2.20×10^{-4}
3	2.21×10^{-4}
4	2.21×10^{-4}
5	2.20×10^{-4}

Based on dynamical response measurements, the herein presented strategy allows updating the model predictions. In particular, the prediction of responses that are not considered in the data used for identification purposes can be updated. To illustrate this feature, the abutment displacements along the x axis are shown in Fig. 5. Specifically, this figure presents the target responses (solid-black lines) as well as their prior and posterior uncertainty represented in terms of 95%-confidence intervals (gray areas). It can be argued that a significant level of uncertainty is present in the prior prediction. Nevertheless, available measurement data can be employed to achieve significant improvements to the predictive capabilities of the model. Indeed, the various lines in the right plots, corresponding to the posterior distribution, are indistinguishable from

one another. That is, the update responses match the target ones. In other words, the posterior distribution identified by the proposed method enables high-quality updated predictions of these unobserved responses.

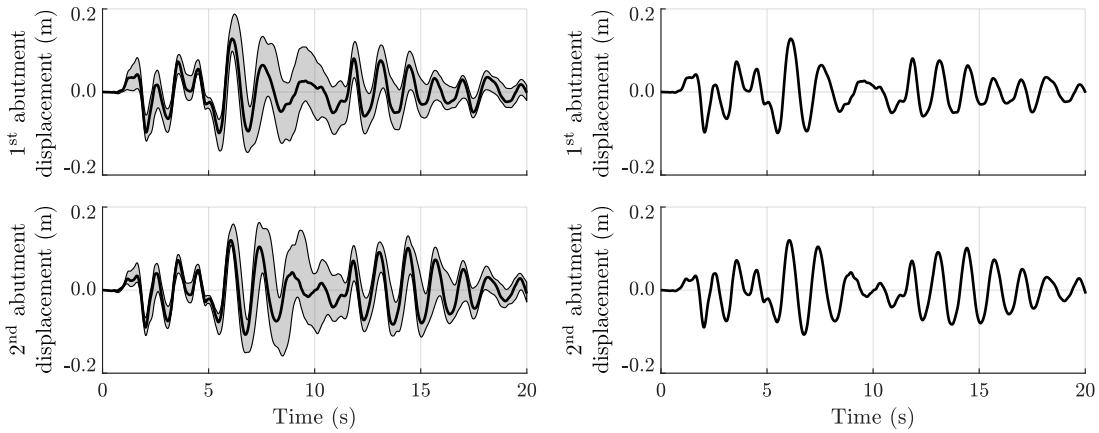

Figure 5. Displacement response at the abutments (x-axis). Target values (black line) and 95%-confidence interval (gray area). Left: Prior distribution. Right: Updated distribution.

Figure 6 presents the value of threshold level, d^*, obtained throughout the different subset simulation levels. It is noted that, within the proposed approach, this quantity is directly related to the likelihood multiplier and is associated with the maximum value of the likelihood function observed during the sampling process. From the figure, it is seen that 10 stages are needed to verify the stopping condition. Moreover, the value of d^* stabilizes roughly after five stages, with a marginal incremental trend in later stages. This indicates the validity of the proposed strategy to select the likelihood multiplier, since the region of the parameter space associated with high values of the likelihood function can be efficaciously sampled. To obtain further insight into the performance of the method, Table 2 reports the estimates of the log-evidence computed from five independent runs. These estimates, which are computed with negligible computational efforts, are very similar between each other. Overall, the preceding findings suggest that the herein reported BUS implementation can be employed to address Bayesian model updating problems associated with complex nonlinear structural systems and dynamical response measurements.

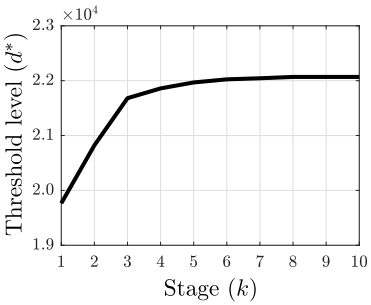

Figure 6. Threshold level in terms of simulation level.

5. Conclusions

An effective implementation of Bayesian updating with structural reliability methods (BUS), suitable for the treatment of dynamic nonlinear structural systems, has been presented. In this setting, posterior samples are obtained as those lying in an especially devised failure domain. Subset simulation, a popular sampling technique for reliability analysis, is considered. Further,

a formulation to determine the likelihood multiplier in an adaptive manner is presented. For improved numerical efficiency, parametric reduced-order models are implemented using the concept of substructure coupling for dynamic analysis. To illustrate the advantages of the herein reported approach, an application example involving a three-dimensional finite element model involving friction-based isolators is studied. In general, the predictive capabilities of the structural dynamical system are enhanced by virtue of available response measurements. Moreover, significant computational efficiency improvements are achieved by the model reduction technique under consideration while ensuring the consistency of the reduced and unreduced models in terms of their relevant dynamical properties. Overall, the findings discussed in this work indicate that the proposed BUS approach can be regarded as a is a potentially useful technique for tackling complex Bayesian model updating problems in realistic scenarios that entail involved nonlinear structural models and measured response data.

Acknowledgments
This work has been supported in part by ANID (National Agency for Research and Development, Chile) and DAAD (German Academic Exchange Service, Germany) under CONCYT-PFCHA/ Doctorado Acuerdo Bilateral DAAD Becas Chile/2018-62180007, and by ANID under grant number 1200087. These supports are gratefully acknowledged by the authors.

6. References

[1] Beck J L and Katafygiotis L S 1998 *Journal of Engineering Mechanics* **124** 455–461
[2] Yuen K V 2010 *Bayesian methods for structural dynamics and civil engineering* (John Wiley & Sons)
[3] Papadimitriou C, Beck J L and Katafygiotis L S 2001 *Probabilistic Engineering Mechanics* **16** 103–113
[4] Metropolis N, Rosenbluth A W, Rosenbluth M N, Teller A H and Teller E 1953 *The Journal of Chemical Physics* **21** 1087–1092
[5] Hastings W K 1970 *Biometrika* **57** 97–109
[6] Ching J and Chen Y C 2007 *Journal of Engineering Mechanics* **133** 816–832
[7] Jin Y F, Yin Z Y, Zhou W H and Horpibulsuk S 2019 *Acta Geotechnica* **14** 1925–1947
[8] Goller B, Broggi M, Calvi A and Schuëller G I 2011 *Finite Elements in Analysis and Design* **47** 739 – 752 ISSN 0168-874X
[9] Betz W, Papaioannou I and Straub D 2016 *Journal of Engineering Mechanics* **142** 04016016
[10] Cheung S H and Beck J L 2009 *Journal of Engineering Mechanics* **135** 243–255
[11] Weng J H, Loh C H and Yang J N 2009 *Journal of Structural Engineering* **135** 1533–1544
[12] Ghorbani E and Cha Y J 2018 *Journal of Sound and Vibration* **420** 21–34
[13] Straub D and Papaioannou I 2015 *Journal of Engineering Mechanics* **141** 04014134
[14] DiazDelaO F A, Garbuno-Inigo A, Au S K and Yoshida I 2017 *Computer Methods in Applied Mechanics and Engineering* **317** 1102–1121 ISSN 0045-7825
[15] Betz W, Beck J L, Papaioannou I and Straub D 2018 *Probabilistic Engineering Mechanics* **53** 14–22
[16] Betz W, Papaioannou I, Beck J L and Straub D 2018 *Computer Methods in Applied Mechanics and Engineering* **331** 72–93
[17] Jerez D J, Jensen H A and Beer M 2022 *Reliability Engineering & System Safety* **225** 108634
[18] Jiang S H, Huang J, Qi X H and Zhou C B 2020 *Engineering Geology* **271** 105597
[19] Liu P, Huang S, Song M and Yang W 2020 *Journal of Civil Structural Health Monitoring* **11** 129–148
[20] Au S K and Beck J L 2001 *Probabilistic Engineering Mechanics* **16** 263–277 ISSN 0266-8920
[21] Hoeting J A, Madigan D, Raftery A E and Volinsky C T 1999 *Statistical Science* **14** 382–401 ISSN 08834237 URL `http://www.jstor.org/stable/2676803`
[22] Zuev K M, Beck J L, Au S K and Katafygiotis L S 2012 *Computers & Structures* **92** 283–296 ISSN 0045-7949 URL `http://www.sciencedirect.com/science/article/pii/S0045794911002720`
[23] Jensen H and Papadimitriou C 2019 *Sub-structure coupling for dynamic analysis* (Springer International Publishing)
[24] Jensen H A, Araya V A, Muñoz A D and Valdebenito M A 2017 *Computer Methods in Applied Mechanics and Engineering* **326** 656–678 ISSN 0045-7825 URL `http://www.sciencedirect.com/science/article/pii/S0045782517300221`
[25] Angelikopoulos P, Papadimitriou C and Koumoutsakos P 2015 *Computer Methods in Applied Mechanics and Engineering* **289** 409–428

[26] Lomiento G, Bonessio N and Benzoni G 2013 *Journal of Earthquake Engineering* **17** 1162–1191
[27] Pastor M, Binda M and Harčarik T 2012 *Procedia Engineering* **48** 543–548